Proc. NIPR Symp. Polar Meteorol. Glaciol., **9**, 54–65, 1995

CHARACTERISTICS OF EVAPORATION FROM SNOW AND TUNDRA SURFACE IN SPITSBERGEN IN THE SNOWMELT SEASON 1993

Yukari TAKEUCHI, Yuji KODAMA and Hironori NAKABAYASHI

Institute of Low Temperature Science, Hokkaido University, Kita-19, Nishi-8, Kita-ku, Sapporo 060

Abstract: Meteorological conditions and evaporation from snow and tundra surfaces were measured in the tundra area in Spitsbergen from the end of May to the end of June in 1993. In this period, three types of ground surface were seen, *i.e.* dry snow, melting snow and snow-free tundra. Clear changes in evaporation as well as the meteorological conditions were seen with the changes in surface condition. During the dry snow period, evaporation predominated at the snow surface and the latent heat loss by evaporation suppressed the snowmelt. During the snowmelt period, the temperature of the snow cover was 0°C from the surface to the bottom, and condensation predominated due to the increase of vapor pressure in the air. The latent heat by condensation contributed to the snowmelt. After the seasonal snow was gone and the meltwater was still abundant at the tundra surface, intense evaporation of about 3.7 mmday^{-1} occurred with the rapid surface temperature increase, while condensation occurred on the remaining snow surface.

1. Introduction

Evaporation from the snow surface and the tundra surface is an important component of the water balance and heat balance in the Arctic region, where annual precipitation is very small and daily global radiation is large during the midnight-sun season. OHMURA (1982) reported that annual evaporation at the tundra surface on Axel Heiberg Island (79°25′ N, 90°45′ W) was estimated at 140 mm, which was equivalent to 80% of annual precipitation. The evaporation rate fluctuates with the change of surface condition such as dry snow, melting snow and the tundra, and shows the largest value immediately after snow had disappears (KANE *et al.*, 1990; OHMURA, 1982; WELLER and HOLMGREN, 1974).

Meteorological conditions and evaporation were measured in the tundra area at Ny-Ålesund (78°50′ N, 11°50′ E), Spitsbergen, for about four weeks from the end of May to the end of June 1993. In this period, three types of surface were seen, *i.e.* dry snow, melting snow and snow-free tundra. The variation of evaporation rate among the three periods is to be reported.

Spitsbergen is the largest island of the Svalbard archipelago situated between latitudes 76°N and 81°N in the Norwegian Arctic (Fig. 1). About 60% of the total area is covered with glaciers and the rest is mostly permafrost area. Temperatures are comparatively high for the high latitude, due largely to the North Atlantic Current, a branch of which flows toward the west coast of Spitsbergen (SAND *et al.*, 1991). Ny-Ålesund looks out on the Kongsfjord, on the north-west coast of Spitsbergen (Fig. 1). Annual mean temperature at Ny-Ålesund is −6°C, while the mean temperature in

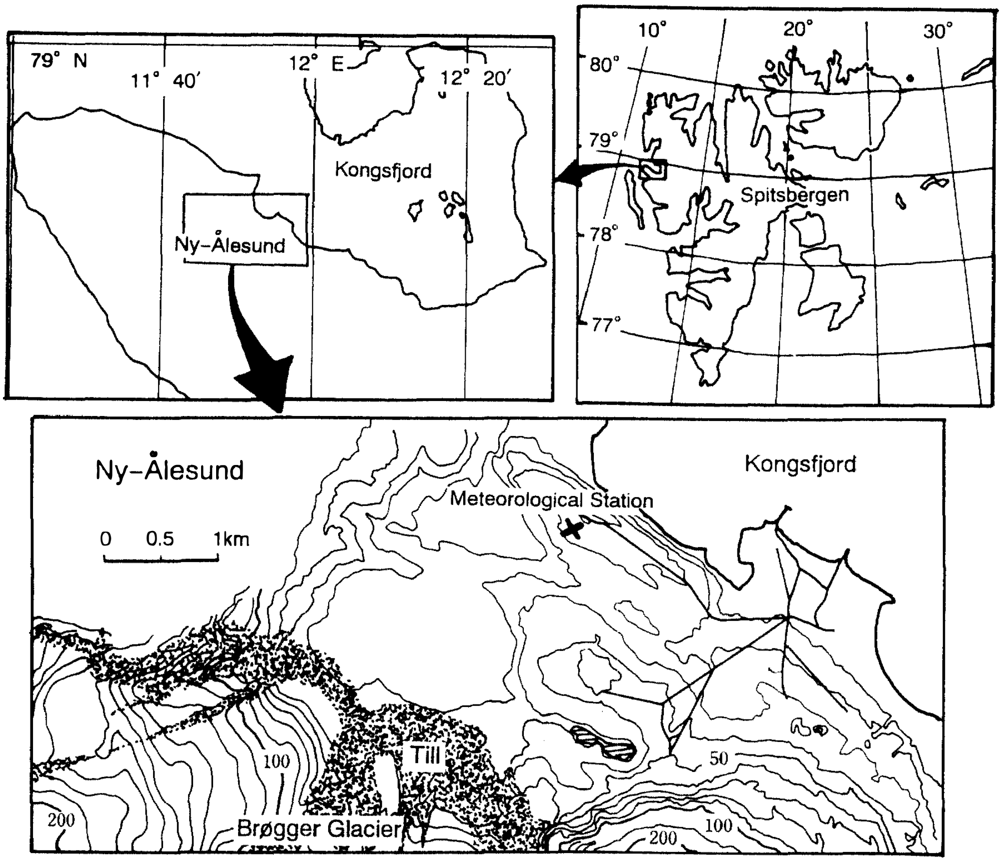

Fig. 1. Maps of Ny-Ålesund, Spitsbergen and observation site. ×: the meteorological station.

July, the warmest month, is approximately 5°C. Annual precipitation ranges from 400 mm to 1000 mm (SKRETTEBERG, 1991). At Ny-Ålesund, the sun is above the horizon all day long from April 18 to August 24.

2. Observation Methods

2.1. Observation site and period

The observation site is shown in Fig. 1. The meteorological station was placed on flat land, about 200 m from the coast and about 2 km from the terminus of Brøgger glacier. Only the continuous measurement of evaporation, which needs alternating current, was made at a point about 100 m from the coast. The observation period was from May 28 to June 22, 1993.

2.2. Meteorological measurements

Air temperature, relative humidity, surface temperature, wind speed and snow temperature were continuously measured and recorded with portable data loggers at the meteorological station. In addition to these, some manual observations, such as snow depth, surface snow density and cloud amount were routinely made at 9 h and 18 h. All instruments were maintained at this time and the height and level of instruments were adjusted when needed. Wind speed was measured at 1 m and 0.1 m above the surface.

Table 1. Meteorological elements.

Elements	Instruments and accuracy	Recording interval
Air temperature (1 m)	Hygrothermometer (with sunshade and ventilation)/0.2℃	30 min (scanning interval: 30 s)
Relative humidity (1 m)	Hygrothermometer (with sunshade and ventilation)/5%	30 min (scanning interval: 30 s)
Surface temperature	Infrared thermometer/±1%	30 min (scanning interval: 30 s)
Snow temperature (5 cm, 10 cm, 20 cm, 50 cm)	Thermistor thermometer/0.2℃	30 min (scanning interval: 30 s)
Wind speed (1 m, 0.1 m)	Three-cup anemometer/±1% Threshold wind speed: 0.2 ms^{-1}	10 min
Global radiation	Solarmeter pyranometer/±1%	30 min (scanning interval: 30 s)
Reflected radiation	Solarmeter pyranometer/±1%	30 min (scanning interval: 30 s)
All wave net radiation	Net radiometer/±5%	30 min (scanning interval: 30 s)
Snow depth	Ablation stakes/±1 mm	Twice a day
Snow density	Snow sampler/±1%	Twice a day
Cloud amount	Visual observation/±15%	Twice a day
Evaporation	Weighing lysimeter/1 g	10 min

Other sensors were set at 1 m height above the surface. A sensor of hygrothermometer was inserted in a double pipe and ventilated by a micro-fan for insulating global radiation. Meteorological elements, instruments and interval of measurement are summarized in Table 1.

2.3. Measurement of evaporation

Evaporation from the snow surface was measured with a weighing lysimeter (Fig. 2). A snow block in a vessel, which was taken from the snow surface without destroying its original structure, was continuously weighed by an electric balance and recorded with a personal computer every 10 min. The capacity of the electric balance is 30 kg and the accuracy is 1 g. The vessel was made of vinyl-chloride and is 46 cm × 40 cm. The snow block was on the mesh in the vessel. The meltwater fell through the mesh and collected in the bottom of the vessel. Owing to this mesh, the snow block in the vessel was not filled with the meltwater. The snow was renewed every two or three days during the dry snow period and every day during the melt period. After seasonal snow disappeared in places on June 20, the cylindrical vessel with a diameter of about 10 cm filled with lichen, soil and water was weighed a few times a day.

2.4. Heat balance computation

The heat balance equation at the snow surface can be written as follows:

$$NR + S + L + C + M = 0, \qquad (1)$$

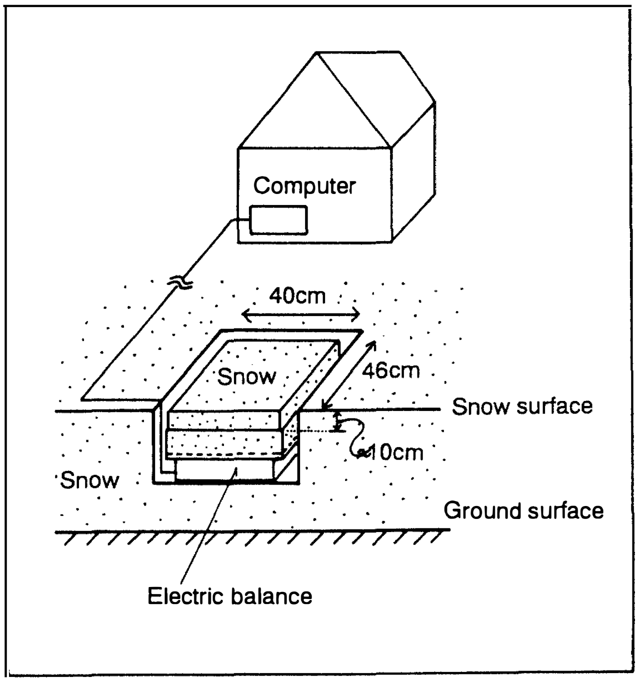

Fig. 2. Schematic diagram of measurement of evaporation from the snow surface with the electric balance.

where NR is the all wave net radiation, S the sensible heat flux, L the latent heat flux, C the conductive heat flux in the snow pack and M the heat for melting. Fluxes toward the surface are regarded as positive, and those away from the surface as negative. NR was measured directly by a net radiometer. The turbulent heat fluxes S and L were obtained from wind speed, air temperature and vapor pressure using bulk aerodynamic approaches (ISHIKAWA *et al.*, 1992). The formulae are

$$S = \rho_a C_p D_H (T_Z - T_0), \quad (2)$$

and

$$L = \rho_a L_e D_E (0.622/P_a)(e_Z - e_0), \quad (3)$$

where ρ_a is the air density (kgm^{-3}), C_p the specific heat of air at constant pressure ($J\,kg^{-1}\,°C^{-1}$), T_Z the air temperature (°C) at height Z, T_0 the surface temperature (°C), L_e the latent heat of vaporization of water (Jkg^{-1}), P_a the atmospheric pressure (hPa), e_Z the vapor pressure (hPa) at height Z, e_0 the vapor pressure (hPa) at the surface, D_H the bulk exchange coefficient for heat (ms^{-1}), and D_E the bulk exchange coefficient for water vapor (ms^{-1}). It is assumed that, under a neutral condition, D_H and D_E are the same as the momentum exchange coefficient given by

$$D_0 = k^2 U_Z [\ln(Z/Z_0)]^{-2}, \quad (4)$$

where k is the von Karman constant (=0.4), U_Z the wind speed (ms^{-1}) at height Z, Z

the measurement height (m), and Z_0 the roughness height (m). When the atmospheric conditions are not neutral, the exchange coefficients should be corrected by using the following stability functions;

$$D = D_0(1-5R_b)^2 \qquad 0<R_b<0.25,$$
$$D = D_0(1-16R_b)^{0.75} \qquad 0>R_b, \tag{5}$$

where R_b is the bulk Richardson Number defined by

$$R_b = g(T_Z - T_0)Z/TU_Z^2\ , \tag{6}$$

where g is the gravitational acceleration (ms^{-2}) and T the mean absolute temperature of air (K).

The roughness height Z_0 is calculated from wind speeds at two heights under neutral conditions ($|R_b| < 0.01$) using the equation,

$$Z_0 = \exp[(U_2 \ln Z_1 - U_1 \ln Z_2)/(U_2 - U_1)]. \tag{7}$$

The mean value of Z_0 was 1.2×10^{-4} m at the snow surface. Since the wind speed profile for snow-free surface could not be measured well, the same value as snow surface was used for Z_0 for the snow-free surface.

The conductive heat flux (C) was calculated from the change of heat stored in the snow layers. That is,

$$C = \sum \Delta S_i, \tag{8}$$

where ΔS_i is the change of heat stored in a certain snow layer i for the time Δt. This is given by

$$\Delta S_i = \rho_i C_{ice} \frac{\Delta T_i}{\Delta t} \cdot d_i\ , \tag{9}$$

where ρ_i is the density of snow (kgm^{-3}), C_{ice} the specific heat of ice ($Jkg^{-1}{}^\circ C^{-1}$), ΔT_i the change of snow temperature (°C) for the time of Δt, and d_i the thickness of the snow layer (m). The ΔS_i were calculated using the snow temperatures measured at the depth of 5 cm, 10 cm, 20 cm and 50 cm from the snow surface. The values of ρ_i were given from the snow pit observation as 350, 370, 380 and 450 (kgm^{-3}) for each layer of 0–5 cm, 5–10 cm, 10–20 cm and 20–50 cm, respectively. C_{ice} was given as a function of ice temperature T (°C) as follows (MAENO, 1986),

$$C_{ice} = 2117 - 7.8\ T(Jkg^{-1}{}^\circ C^{-1}). \tag{10}$$

The heat for melting (QM) was given from the measurement of snow surface lowering by stakes as follows:

$$QM = \rho_s L_m h, \tag{11}$$

where ρ_s is the snow surface layer density (kgm^{-3}), L_m the latent heat for melting (J kg^{-1}), and h the amount of snow surface lowering (m). Although ρ_s should be the dry density of surface snow, the wet density was taken as ρ_s in this study following KOJIMA (1971). The values of ρ_s were measured at 9 h and 18 h every day.

3. Measurement Results and Discussion

3.1. Meteorological features

Variations in snow depth and major meteorological elements observed during the observation period are shown in Fig. 3. Snow cover of about 40 cm existed on May 28

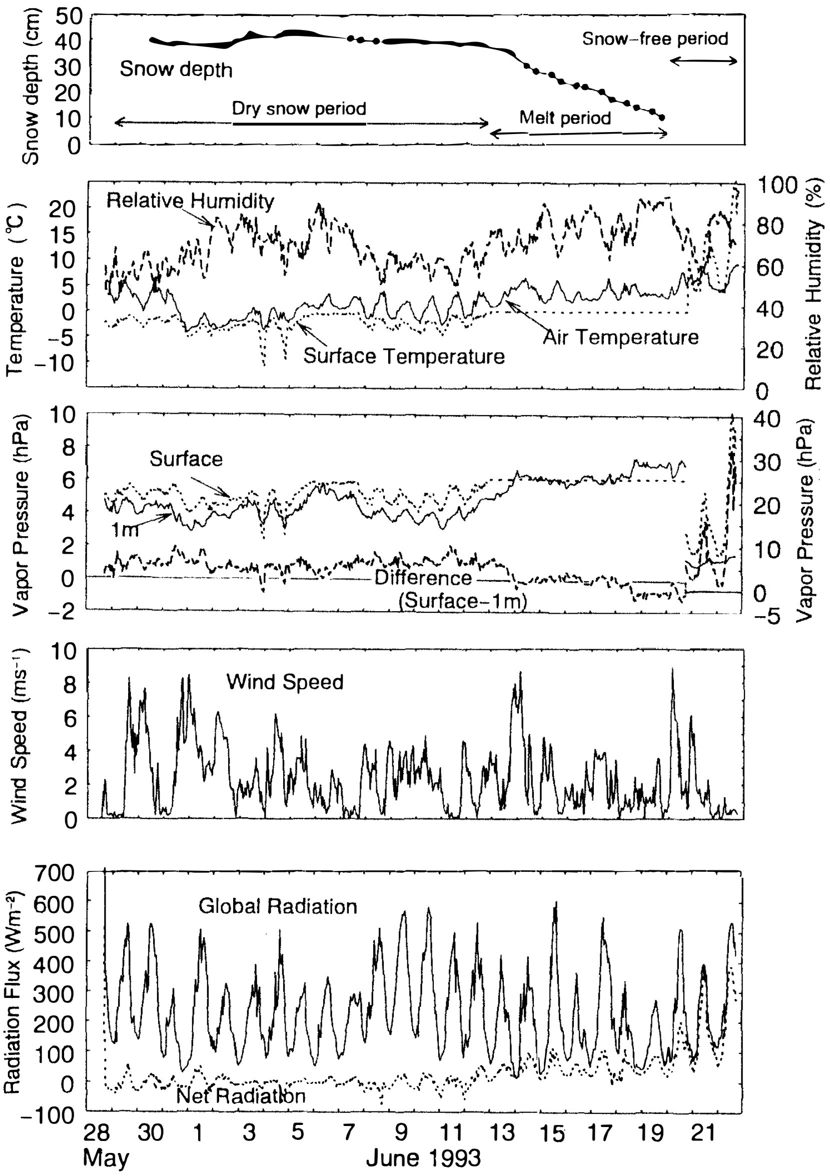

*Fig. 3. Variations in major meteorological elements during the observation period. *Note that the right axis is used for the vapor pressure on June 21 and 22.*

Table 2. Means and extremes of meteorological elements obtained at Ny-Ålesund for each observation period.

Period* / Meteorological elements	Dry snow period			Melt period			Snow-free period		
	Max.	Min.	Av.	Max.	Min.	Av.	Max.	Min.	Av.
Surface temperature (℃)	−0.3	−10.8	−2.5	0.0	0.0	0.0	25.2	3.8	10.8
Air temperature (℃)	6.4	−4.1	0.5	6.6	0.9	3.6	9.4	3.2	6.0
Relative humidity (%)	90.0	45.1	65.4	93.1	62.6	78.7	91.5	56.2	73.8
Vapor pressure (hPa)	5.8	2.9	4.1	7.4	4.8	6.2	8.3	5.6	6.9
Difference of vapor pressure** (hPa)	2.0	−0.9	0.9	1.3	−1.3	−0.1	32.6	0.0	9.2
Wind speed (ms^{-1})	8.5	0.0	2.5	8.7	0.1	2.2	8.9	0.0	2.0
Global radiation (Wm^{-2})	716.4	29.5	252.8	654.5	14.7	193.0	695.4	63.0	264.4
Net radiation (Wm^{-2})	63.0	−71.3	0.1	108.1	−13.8	43.3	484.5	16.6	157.5
Daily global radiation ($MJm^{-2}day^{-1}$)	30.8	15.4	21.7	25.1	11.9	16.7	20.1	19.5	19.8
Daily net radiation ($MJm^{-2}day^{-1}$)	1.3	−1.6	0.0	4.4	2.9	3.7	14.6	8.3	11.5

* Period; Dry snow period: May 28–June 12. Melt period: June 13–19. Snow-free period: June 20–22.
** Surface − 1 m

when the observations started. The snow depth did not decrease by melting before June 12. After June 13, the snow rapidly melted, disappearing on June 20. Clear changes in the meteorological factors were seen with the changes in surface condition when the snowmelt period started and finished. Thus, the observation period was separated into three periods as "dry snow period" (May 28–June 12), "melt period" (June 13–19), "snow-free period" (June 20–22). Extreme and mean values of major meteorological elements during each period are shown in Table 2. Vapor pressure at the surface was regarded as the saturated vapor pressure of ice at the surface temperature.

During the dry snow period, surface temperature fluctuated below 0°C and air temperature was around 0°C. Vapor pressure at the surface was larger than that at 1 m height, evaporation being prominent. The net radiation fluctuated near zero nevertheless the global radiation did not decrease to zero due to the midnight-sun.

During the melt period, the surface temperature was fixed at 0°C and air temperature was always above 0°C. Vapor pressure became larger than that before the melt period and it larger at 1 m than at the surface, which means that condensation dominated. The global radiation was a little smaller than that before the melt period due to larger cloud amount, while the net radiation increased substantially, being above zero all day long. The increase of net radiation was caused by the increase of atmospheric radiation as well as the decrease of albedo, the means of which were 0.80 and 0.69 respectively during dry snow and melt periods (NAKABAYASHI *et al*., 1994).

After the snow disappeared at the meteorological station, surface temperature suddenly rose, which caused large vapor pressure at the surface; the difference of vapor pressure between the surface and 1 m changed to positive and became larger than ten times that for the snow surface. The net radiation also increased remarkably, to values about three times as that of the melt period because of the decrease of the mean albedo from 0.69 to 0.15. There was little change in wind speed or global radiation.

3.2. Characteristics of the heat balance

The heat for snowmelt calculated from the heat balance method by eq. (1) is compared with the heat obtained from snow surface lowering using eq. (11), as shown in Fig. 4. Because of snowfall, the results of stakes 1 and 2 showed negative values on June 2, 3 and 4. These values do not mean the heat for snowmelt. During the dry snow period, the heat for snowmelt was nearly zero; during the melt period, both values agree

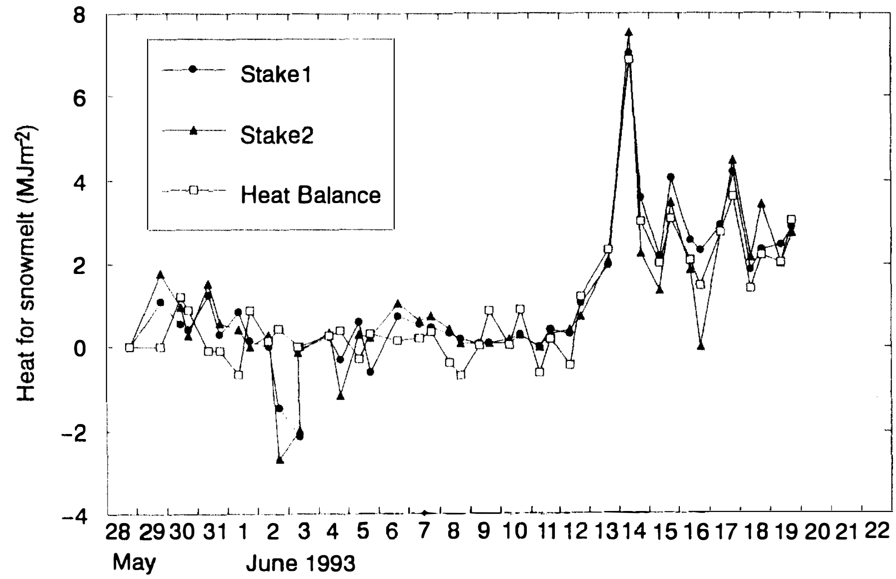

Fig. 4. Comparison of the heat needed for snowmelt calculated by the heat balance method with that measured by two stakes at the meteorological station.

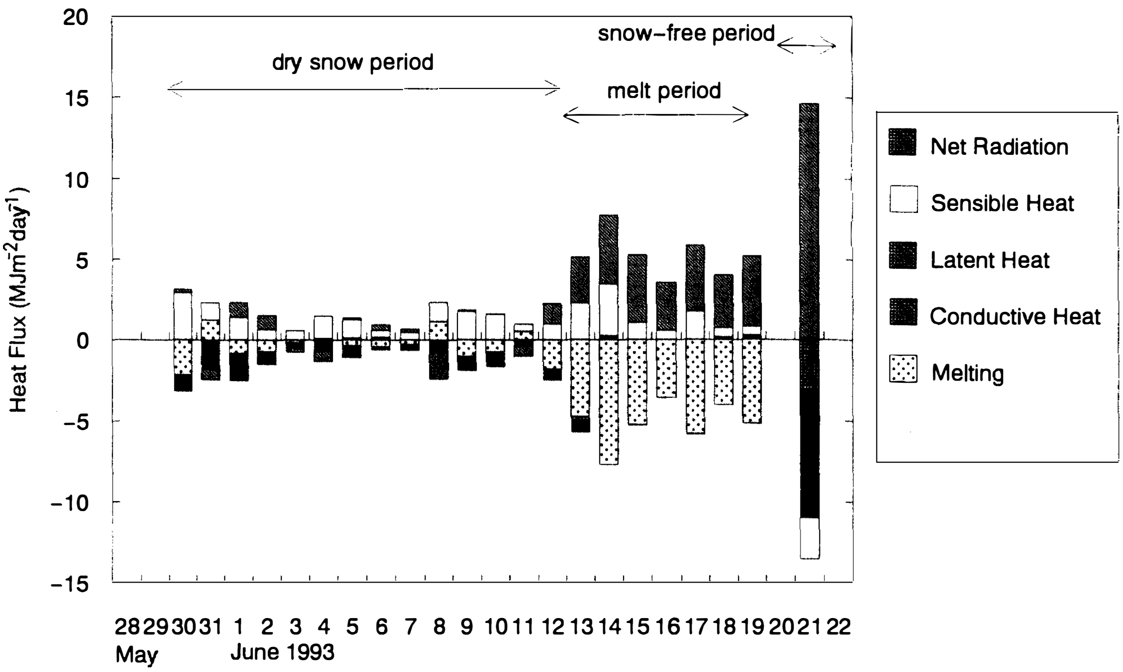

Fig. 5. Daily values of the heat balance components.

well with each another, which means that the methods of heat balance computation have good accuracy (mean error is 7%) to reproduce the heat for snowmelt.

Daily values of heat balance components on the surface are shown in Fig. 5. Clear differences in heat balance components were seen among the periods: dry snow, melt and snow-free period. During the dry snow period, the latent heat was lost by evaporation and the same order of sensible heat was taken from the air. Depending on weather conditions, the net radiation showed positive and negative values, but its amount was relatively small. When the net radiation was positive, surface snow melting occurred, but the amount was small and the temperature of the snow cover was below 0°C. The conductive heat flux was positive but much smaller than the turbulent heat flux.

During the melt period, the net radiation was remarkably large, more than half of the total heat source. The latent heat flux was small but positive after June 14, which means that condensation predominated. The conductive heat flux was zero because the temperature of the snow cover became 0°C from the surface to the bottom. The net radiation, sensible and latent heat fluxes were all heat sources for snowmelt.

During the snow-free period, the net radiation increased to about three times that of the melt period. The sensible heat flux changed to negative due to the surface temperature increase. The latent heat flux also changed to negative, showing intense evaporation. The residual was regarded as conductive heat flux to the ground.

3.3. Characteristics of evaporation

Hourly values of the evaporation or condensation at the snow surface measured by a weighing lysimeter are shown in Fig. 6. Evaporation predominated during the dry snow period, while condensation predominated during the melt period. This was due to increase of vapor pressure in the atmosphere accompanied with advection of an warm air mass from lower latitude (NAKABAYSHI *et al.*, 1994), while the surface vapor

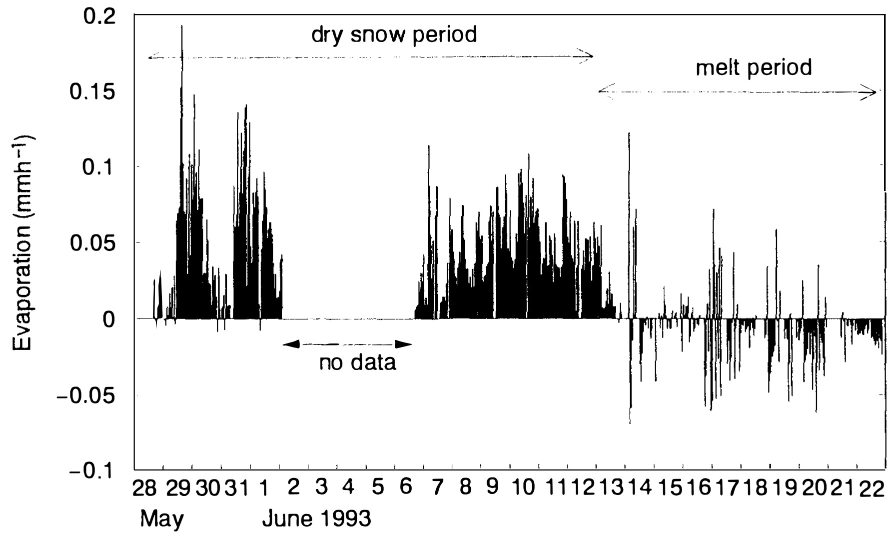

Fig. 6. Evaporation from snow surface measured with the weighing lysimeter.

pressure was fixed to the saturation value 0°C. The sense of evaporation measured with the weighing lysimeter coincided with that calculated by the bulk aerodynamic method (eq. (3) and others), but the evaporation rate of the former was always larger than the latter. Although frost sometimes formed on the outside of the vessel and evaporated, it was confirmed that the amount was much smaller than evaporation or condensation from/to the snow surface. Since the height of the snow block in the vessel was higher than the edge of the vessel as shown in Fig. 2, the edge of the vessel did not receive the global radiation. It also can be considered that there was little evaporation or condensation from/to the side of the snow block, since the snow block was set close to the surrouding snow. The electric balance was checked for dependence on environmental temperature and it was not affected by sub-zero temperature (as low as -5°C) although this was not guaranteed by the maker. The reason for the difference between the measured and calculated values is not clear at present. As shown in Fig. 4, the values

Table 3. Evaporation from the tundra surface immediately after the snow melt period.

Period	Evaporation rate (mmh^{-1})
June 20, 1000–21, 0020	0.17
21, 0020–21, 0920	0.11
21, 0920–21, 2220	0.09
21, 2220–22, 1100	0.08
22, 1110–22, 1345	0.15
22, 1345–23, 0030	0.12
23, 0030–23, 0845	0.06
June 21, 0020–23, 0030	7.4 (mm)
Average	3.7 ($mmday^{-1}$)

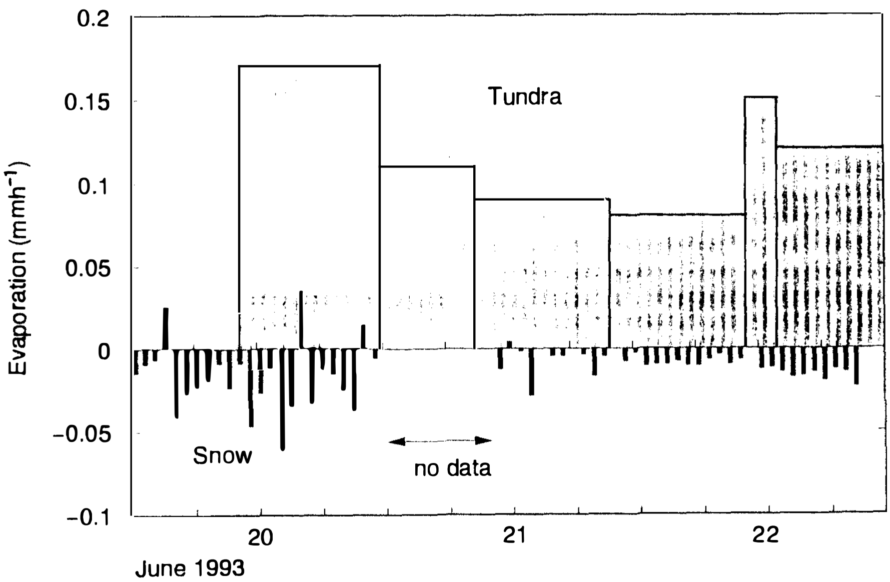

Fig. 7. Evaporation from tundra and snow surface around tundra immediately after snow disappearance.

calculated by the bulk aerodynamic method could reproduce the heat for snowmelt, therefore the calculated values may be reasonable in this study.

After June 20, evaporation from the tundra surface was measured with an evaporation pan at the site where snow cover had disappeared partially, while measurement of evaporation from the snow surface was continued at the site where snow cover still remained. These measurement results are shown in Table 3 and Fig. 7. Evaporation of about 3.7 $mmday^{-1}$ was measured from the tundra surface in the evaporation pan. This value can be regarded as reasonable comparing to the results of measurement or estimation of summer evaporation in the arctic area summarized by KANE *et al.* (1990), considering that the annual largest evaporation occurred immediately after snow disappearance in the arctic area (KANE *et al.*, 1990; OHMURA, 1982; WELLER and HOLMGREN, 1974). On the other hand, during this period, condensation occurred at the snow surface of the weighing lysimeter (Fig. 6). It was suggested accordingly that during the period when the snow cover disappeared partially and the tundra surface began to appear, intense evaporation occurred on the tundra surface, while condensation occurred on the surrounding snow surface.

4. Summary

According to the meteorological conditions and evaporation measurements in the tundra area on Spitsbergen during the snowmelt season 1993, the characteristics of evaporation from the snow and tundra surfaces are summarized as follows:

1) During the dry snow period, evaporation predominated on the snow surface. The latent heat flux lost by evaporation was equivalent to the sensible heat flux and suppressed the snowmelt.

2) During the melt period, condensation predominated on the snow surface due to the increase of vapor pressure in air. The latent heat by condensation was small but contributed to promote snowmelt.

3) When snow cover disappeared partially and tundra surface filled with meltwater appeared, the surface temperature of the tundra increased rapidly and intense evaporation from the tundra surface, about 3.7 $mmday^{-1}$ in average, was observed, whereas the condensation occurred on the partial snow surface around the tundra.

Acknowledgments

The authors wish to thank Drs. S. USHIO and S. KUDOH, Arctic Environment Research Center, National Institute of Polar Research for their cooperation in the observations at Ny-Ålesund.

References

ISHIKAWA, N., OWENS, I. F. and STURMAN, A. P. (1992): Heat balance characteristics during fine periods on the lower parts of the Franz Josef Glacier, South Westland, New Zealand. Int. J. Climatol., **12**, 397–410.

KANE, D. L., GIECK, R. E. and HINZMAN, L. D. (1990): Evapotranspiration from a small Alaskan Arctic watershed. Nordic Hydrol., **21**, 253–272.

KOJIMA, K. (1971): Sekisetsu-hyômensô no netsu-shûshi to yûsetsu no kansoku rei. Seppyô, **33**, 260–269.

MAENO, N. (1986): Seppyo no Kôzô to Bussei, ed. by N. MAENO and M. FUKUDA. Tokyo, Kokon Shoin, 81–130 (Kiso Seppôgaku Kôza I).

NAKABAYASHI, H., KODAMA, Y. and TAKEUCHI, Y. (1994): Spitsbergen no yûsetsu katei (Process of snowmelt in Spitsbergen). Teion Kagaku, Butsuri-hen (Low Temp. Sci., Ser. A, Phys.), **53**, 11–22.

OHMURA, A. (1982): Evaporation from the surface of the Arctic tundra on Axel Heiberg Island. Water Resour. Res., **18**, 291–300.

SAND, K., HAGEN, J. O., REPP, K. and BERNTSEN, E. (1991): Climate related research in Svalbard. Arctic Hydrology, Present and Future Tasks, Hydrology of Svalbard-Hydrological Problems in Cold Climate, ed. by Y. GJESSING *et al.* Oslo, Norwegian National Committee for Hydrology, 203–217 (NHK Report No. 23).

SKRETTEBERG, R. (1991): Discharge measurements structures under Arctic conditions, Design and construction considerations. Arctic Hydrology, Present and Future Tasks, Hydrology of Svalbard-Hydrological Problems in Cold Climate, ed. by Y. GJESSING *et al.* Oslo, Norwegian National Committee for Hydrology, 167–174 (NHK Report No. 23).

WELLER, G. and HOLMGREN, B. (1974): The microclimates of the arctic tundra. J. Appl. Meteorol., **13**, 854–862.

(Received January 4, 1995; Revised manuscript received May 8, 1995)